

January 2005

# Shear Stress in Smooth Rectangular Open-Channel Flows

Junke Guo

*University of Nebraska - Lincoln, jguo2@unl.edu*

Pierre Y. Julien

*Colorado State University*

Follow this and additional works at: <http://digitalcommons.unl.edu/civilengfacpub>



Part of the [Civil Engineering Commons](#)

---

Guo, Junke and Julien, Pierre Y., "Shear Stress in Smooth Rectangular Open-Channel Flows" (2005). *Civil Engineering Faculty Publications*. 1.

<http://digitalcommons.unl.edu/civilengfacpub/1>

This Article is brought to you for free and open access by the Civil Engineering at DigitalCommons@University of Nebraska - Lincoln. It has been accepted for inclusion in Civil Engineering Faculty Publications by an authorized administrator of DigitalCommons@University of Nebraska - Lincoln.

# Shear Stress in Smooth Rectangular Open-Channel Flows

Junke Guo<sup>1</sup> and Pierre Y. Julien<sup>2</sup>

**Abstract:** The average bed and sidewall shear stresses in smooth rectangular open-channel flows are determined after solving the continuity and momentum equations. The analysis shows that the shear stresses are function of three components: (1) gravitational; (2) secondary flows; and (3) interfacial shear stress. An analytical solution in terms of series expansion is obtained for the case of constant eddy viscosity without secondary currents. In comparison with laboratory measurements, it slightly overestimates the average bed shear stress measurements but underestimates the average sidewall shear stress by 17% when the width–depth ratio becomes large. A second approximation is formulated after introducing two empirical correction factors. The second approximation agrees very well ( $R^2 > 0.99$  and average relative error less than 6%) with experimental measurements over a wide range of width–depth ratios.

**DOI:** 10.1061/(ASCE)0733-9429(2005)131:1(30)

**CE Database subject headings:** Open channel flow; Boundary shear; Shear stress; Secondary flow; Velocity.

## Introduction

The problem of separating the bed shear stress and the side-wall shear stress is very important in almost all studies of open-channel flows. For example, one must know boundary shear stress to study a velocity profile (Guo and Julien 2001; Babaeyan-Koopaei et al. 2002). One must separate the bed shear stress from the total shear stress to estimate bed-load transport in open-channel flows. Similarly, to study channel migration or to prevent bank erosion, one must know the side-wall shear stress. Moreover, a side-wall correction procedure is often needed in laboratory flume studies of velocity profiles, bedform resistance and sediment transport (Julien 1995; Cheng 2002; Berlamont et al. 2003). Wall shear stress measurement techniques were also recently reviewed by Bocchiola et al. (2003). This paper aims at determining the average boundary shear stress in smooth rectangular open channels from continuity and momentum equations.

Seven decades ago, Leighly (1932) proposed the idea of using conformal mapping to study the boundary shear stress distribution in open-channel flows. He pointed out that, in the absence of secondary currents, the boundary shear stress acting on the bed must be balanced by the downstream component of the weight of water contained within the bounding orthogonals. This idea has not rendered any conclusive results (Graf 1971, p. 107), though Lundgren and Jonsson (1964) extended the logarithmic law to a parabolic cross-sectional open channel and proposed a method to

determine the shear stress and velocity distribution. Chiu and his associates (Chiu and Lin 1983; Chiu and Chiou 1986) investigated the complex interaction between primary and secondary flows, shear stress distribution, channel characteristics (roughness, slope, and geometry), and other related variables in open channels. The difficulty is that the calculation of boundary shear stress requires the knowledge of velocity profile.

Keulegan (1938) and Johnson (1942) contributed to the early development of this subject, and Einstein's (1942) hydraulic radius separation method (Chien and Wan 1999, p. 266) is still widely used in laboratory studies and engineering practice. Einstein divided a cross-sectional area into two areas  $A_b$  and  $A_w$ , as shown in Fig. 1. He assumed that the downstream component of the fluid weight in area  $A_b$  is balanced by the resistance of the bed. Likewise, the downstream component of the fluid weight in area  $A_w$  is balanced by the resistance of the two side walls. There is no friction at the interface between the two areas  $A_b$  and  $A_w$ . In terms of energy, the potential energy provided by area  $A_b$  is dissipated by the channel bed, and the potential energy provided by area  $A_w$  is dissipated by the two side walls. Following this idea, Yang and Lim (1997, 1998) recently proposed an analytical method to delineate the two areas. However, their method is inconvenient for applications because of its implicit and segmental form (Guo 1999) except without considering the effects of secondary currents.

Since the 1960s, several experimental studies have been reported by Cruff (1965), Ghosh and Roy (1970), Kartha and Leutheusser (1970), Myers (1978), Knight and Macdonald (1979), Knight (1981), Noutsopoulos and Hadjipanous (1982), Knight et al. (1984), Hu (1985), and others. Knight and his associates collected a great deal of experimental data about the effect of the side walls at different width–depth ratios. With these data, they proposed several empirical relations which are very helpful in the studies of open-channel flow and sediment transport.

Starting with the continuity and momentum equations for a steady uniform flow, the objective of this paper is first to formulate a theoretical basis for the boundary shear stress in rectangular open channels. As a first approximation, the boundary shear stress will be solved by using conformal mapping, after neglecting secondary currents and assuming a constant eddy viscosity. A second approximation is then presented by introducing two lumped em-

<sup>1</sup>Assistant Professor, Dept. of Civil Engineering, Univ. of Nebraska–Lincoln, PKI 110 S. 67th St., Omaha, NE 68182; and, Affiliate Faculty, The State Key Lab of Water Resources and Hydropower Engineering Sciences, Wuhan Univ., Wuhan, Hubei 430072, PRC.

<sup>2</sup>Professor, Engineering Research Center, Dept. of Civil Engineering, Colorado State Univ., Fort Collins, CO 80523. E-mail: pierre@engr.colostate.edu

Note. Discussion open until June 1, 2005. Separate discussions must be submitted for individual papers. To extend the closing date by one month, a written request must be filed with the ASCE Managing Editor. The manuscript for this paper was submitted for review and possible publication on January 29, 2002; approved on August 9, 2004. This paper is part of the *Journal of Hydraulic Engineering*, Vol. 131, No. 1, January 1, 2005. ©ASCE, ISSN 0733-9429/2005/1-30–37/\$25.00.

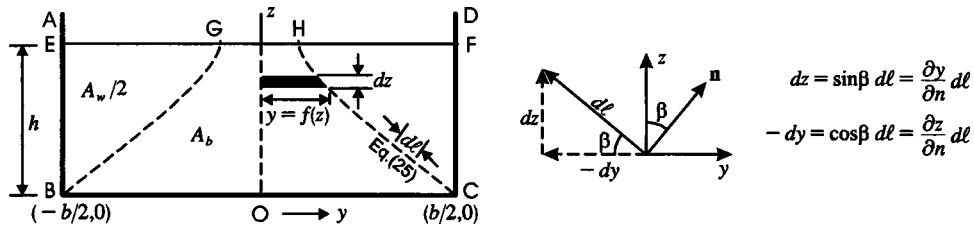


Fig. 1. Partition of cross-sectional area for bed shear stress and side-wall shear stress

pirical correction factors for the effects of secondary currents, variable eddy viscosity and other possible effects. Both approximations will be compared with the existing experimental data. Finally, the implication to flume velocity profile studies will be briefly discussed.

### Theoretical Analysis

Consider steady uniform flow in a rectangular open channel. The flow direction defines the axis  $x$ , and the cross-sectional plane  $y-z$  is shown in Fig. 2. Accordingly, the main flow velocity in the axis  $x$  is denoted as  $u$ , and the secondary currents in the plane  $y-z$  are  $v$  and  $w$ , respectively. One can show that the corresponding continuity and momentum equations in the flow direction  $x$  are

$$\frac{\partial v}{\partial y} + \frac{\partial w}{\partial z} = 0 \quad (1)$$

$$\rho \left( v \frac{\partial u}{\partial y} + w \frac{\partial u}{\partial z} \right) = \rho g S + \frac{\partial \tau_{yx}}{\partial y} + \frac{\partial \tau_{zx}}{\partial z} \quad (2)$$

in which  $\rho$  = mass density of water;  $g$  = gravitational acceleration;  $S$  = channel slope; and  $\tau_{yx}$  and  $\tau_{zx}$  = shear stresses in the flow direction  $x$  applied on the  $z-x$  plane and the  $y-x$  plane, respectively. The convective accelerations on the left-hand side of Eq. (2) account for secondary currents. The first term on the right-hand side is the gravity component in the flow direction, and the other two are net shear stresses applied on a differential element of fluid. The momentum equation in terms of shear stress is used since this study focuses on boundary shear stresses instead of velocity distributions.

Multiplying Eq. (1) by  $\rho u$  and adding it to the left-hand side of Eq. (2) gives

$$\frac{\partial(\rho uv)}{\partial y} + \frac{\partial(\rho uw)}{\partial z} = \rho g S + \frac{\partial \tau_{yx}}{\partial y} + \frac{\partial \tau_{zx}}{\partial z} \quad (3)$$

The corresponding volume integral equation to the above equation is

$$\int_V \left[ \frac{\partial(\rho uv)}{\partial y} + \frac{\partial(\rho uw)}{\partial z} \right] dV = \int_V \rho g S dV + \int_V \left( \frac{\partial \tau_{yx}}{\partial y} + \frac{\partial \tau_{zx}}{\partial z} \right) dV \quad (4)$$

in which  $V$  = arbitrary volume with surface  $A$ . Applying Gauss's theorem to the left-hand side and the second integration on the right hand side results in

$$\int_A \rho u \left( v \frac{\partial y}{\partial n} + w \frac{\partial z}{\partial n} \right) dA = \rho g V S + \int_A \left( \tau_{yx} \frac{\partial y}{\partial n} + \tau_{zx} \frac{\partial z}{\partial n} \right) dA \quad (5)$$

in which  $\partial y / \partial n$  = cosine of the angle between the axis  $y$  and the normal vector  $\mathbf{n}$  pointing outside of the control volume; and similarly  $\partial z / \partial n$  = cosine of the angle between the axis  $z$  and the normal vector  $\mathbf{n}$ . The left-hand side of the above equation is the net momentum flux out of the control surface  $A$ . The first term of the right-hand side is the gravity component of the control volume, and the second term of the right-hand side is the shear force on the control surface  $A$ . Eq. (5) will be used to formulate the boundary shear stress equation.

### Average Bed Shear Stress Equation

Consider a control volume  $BCHGB$  in Fig. 1 that has a unit length in the flow direction  $x$ . The delimitations  $BG$  and  $CH$  are symmetric with respect to the axis  $z$ . The momentum flux in Eq. (5) is then

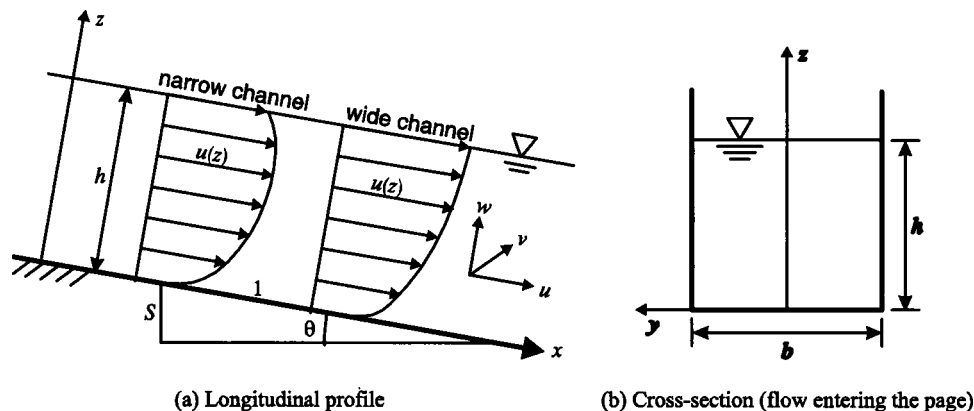


Fig. 2. Coordinate system in open-channel flows

$$\int_A \rho u \left( v \frac{\partial y}{\partial n} + w \frac{\partial z}{\partial n} \right) dA = \int_{BC} + \int_{CH} + \int_{HG} + \int_{GB} \quad (6)$$

in which

$$\int_{BC} = \int_{BC} \rho u \left( v \frac{\partial y}{\partial n} + w \frac{\partial z}{\partial n} \right) dA = 0 \quad (7)$$

because  $v=w=0$  (no-slip condition),  $\partial y/\partial n=0$ , and  $\partial z/\partial n=-1$  at the channel bed

$$\begin{aligned} \int_{GB} &= \int_{CH} = \int_{CH} \rho u \left( v \frac{\partial y}{\partial n} + w \frac{\partial z}{\partial n} \right) dA \\ &= \int_{CH} \rho u \left( v \frac{\partial y}{\partial n} + w \frac{\partial z}{\partial n} \right) dl \\ &= \int_{CH} \rho u (v dz - w dy) \end{aligned} \quad (8)$$

because  $dz=\partial y/\partial n \cdot dl$ ,  $-dy=\partial z/\partial n \cdot dl$ ,  $dA=dl \cdot 1=dl$ , in which  $dl$ =differential length along delimitation  $CH$ , shown in Fig. 1, "1" means a unit length in the flow direction  $x$ , and the symmetric condition has been used for the integration over the curve  $GB$ ; and

$$\int_{HG} = \int_{HG} \rho u \left( v \frac{\partial y}{\partial n} + w \frac{\partial z}{\partial n} \right) dA = 0 \quad (9)$$

because  $\partial y/\partial n=0$ ,  $\partial z/\partial n=1$ ,  $v \neq 0$ , and  $w=0$  at the free surface. Substituting Eqs. (7)–(9) into Eq. (6) yields

$$\int_A \rho u \left( v \frac{\partial y}{\partial n} + w \frac{\partial z}{\partial n} \right) dA = 2 \int_{CH} \rho u (v dz - w dy) \quad (10)$$

The gravity term in Eq. (5) becomes

$$\rho g S V = \rho g S A_b \quad (11)$$

in which  $V=A_b \cdot 1=A_b$  that is the flow area corresponding to the channel bed.

The term of shear force in Eq. (5) becomes

$$\int_A \left( \tau_{yx} \frac{\partial y}{\partial n} + \tau_{zx} \frac{\partial z}{\partial n} \right) dA = \int_{BC} + \int_{CH} + \int_{HG} + \int_{GB} \quad (12)$$

in which

$$\int_{BC} = \int_{BC} \left( \tau_{yx} \frac{\partial y}{\partial n} + \tau_{zx} \frac{\partial z}{\partial n} \right) dA = -\bar{\tau}_b b \quad (13)$$

because  $\partial y/\partial n=0$ ,  $\partial z/\partial n=-1$ ,  $\tau_{zx}=\bar{\tau}_b$  (note that  $\tau_{zx}$  is positive in the negative direction of a negative plane  $y-x$ , according to the sign conventions of shear stresses) that is the average bed shear stress, and the area of the channel bed is  $A=b \cdot 1=b$

$$\begin{aligned} \int_{GB} &= \int_{CH} = \int_{CH} \left( \tau_{yx} \frac{\partial y}{\partial n} + \tau_{zx} \frac{\partial z}{\partial n} \right) dA \\ &= \int_{CH} \left( \tau_{yx} \frac{\partial y}{\partial n} + \tau_{zx} \frac{\partial z}{\partial n} \right) dl \\ &= \int_{CH} (\tau_{yx} dz - \tau_{zx} dy) \end{aligned} \quad (14)$$

because  $dz=\partial y/\partial n \cdot dl$  and  $-dy=\partial z/\partial n \cdot dl$ ; and

$$\int_{HG} = \int_{HG} \left( \tau_{yx} \frac{\partial y}{\partial n} + \tau_{zx} \frac{\partial z}{\partial n} \right) dA = 0 \quad (15)$$

because  $\partial y/\partial n=0$ ,  $\partial z/\partial n=1$ , and  $\tau_{yx}=\tau_{zx}=0$  at the free surface. Substituting Eqs. (13)–(15) into Eq. (12) gives

$$\int_A \left( \tau_{yx} \frac{\partial y}{\partial n} + \tau_{zx} \frac{\partial z}{\partial n} \right) dA = -\bar{\tau}_b b + 2 \int_{CH} (\tau_{yx} dz - \tau_{zx} dy) \quad (16)$$

Substituting Eqs. (10), (11), and (16) into (5) produces

$$2 \int_{CH} \rho u (v dz - w dy) = \rho g S A_b - \bar{\tau}_b b + 2 \int_{CH} (\tau_{yx} dz - \tau_{zx} dy) \quad (17)$$

which results in

$$\bar{\tau}_b = \frac{\rho g S A_b}{b} - \frac{2}{b} \int_{CH} \rho u (v dz - w dy) + \frac{2}{b} \int_{CH} (\tau_{yx} dz - \tau_{zx} dy) \quad (18)$$

This is the theoretical equation of the average bed shear stress. The first term of the right-hand side describes the gravitational component. The second term is associated with secondary currents and the last term represents the shear stress at the interface  $CH$ .

### Average Side-Wall Shear Stress Equation

Similarly, the average side-wall shear stress  $\bar{\tau}_w$  can be formulated by applying Eq. (5) to the control volume  $BGEB$  or  $CFHC$  in Fig. 1. However, a short way to derive the average side-wall shear stress is to consider the overall force balance in the flow direction. That is

$$2h\bar{\tau}_w + b\bar{\tau}_b = \rho g b h S \quad (19)$$

in which the first term on the left-hand side is the shear force on the two side walls, the second term is the shear force on the channel bed, and the right-hand side is the component of water gravity in the flow direction. Applying Eq. (18) in Eq. (19) gives the average side-wall shear stress as

$$\begin{aligned} \bar{\tau}_w &= \frac{\rho g b h S - b\bar{\tau}_b}{2h} \\ &= \frac{\rho g S A_w}{2h} + \frac{1}{h} \int_{CH} \rho u (v dz - w dy) - \frac{1}{h} \int_{CH} (\tau_{yx} dz - \tau_{zx} dy) \end{aligned} \quad (20)$$

in which  $A_w=bh-A_b$  has been used.

To summarize Eqs. (18) and (20), one can see that the boundary shear stress consists of three components: the first term is the

gravity contribution, the second term is the effect of secondary currents, and the third term is the effect of fluid shear stresses that, in turn, reflect the effect of eddy viscosity in turbulent flows. The first term is the dominant term with small contributions from the second and third terms on the right-hand side of Eqs. (18) and (20). Note that although Eqs. (18) and (20) are here derived for smooth rectangular open channels, they are valid for all types of cross sections as long as  $BG$  and  $CH$  are symmetrical.

### First Approximation Without Secondary Currents

To estimate the boundary shear stresses from Eqs. (18) and (20), one must know the main velocity  $u$  and secondary currents  $v$  and  $w$ , the shear stresses  $\tau_{yx}$  and  $\tau_{zx}$ , and the integration path  $CH$ . On the other hand, to solve for velocity field, one must know the boundary shear stresses. This interaction between velocity and shear stress makes the solution of boundary shear stresses or velocity profiles very complicated, as shown by Chiu and Chiou (1986). As a first approximation, one may neglect the effects of secondary currents and the fluid shear stresses. Thus, Eq. (18) becomes

$$\bar{\tau}_b = \frac{\rho g S A_b}{b} \quad (21a)$$

or

$$\frac{\bar{\tau}_b}{\rho g h S} = \frac{A_b}{bh} \quad (21b)$$

and Eq. (20) becomes

$$\bar{\tau}_w = \frac{\rho g S A_w}{2h} \quad (22a)$$

or

$$\frac{\bar{\tau}_w}{\rho g h S} = \frac{A_w}{2h^2} \quad (22b)$$

The remaining problem is to find the areas  $A_b$  and  $A_w$ , which is equivalent to find the delimitations  $BG$  and  $CH$  in Fig. 1.

### Delimitations $BG$ and $CH$

The first approximation assumes that: (1) secondary currents are neglected; and (2) the eddy viscosity  $\nu_t$  is constant. Applying these two assumptions to Eq. (2) gives

$$\frac{\partial^2 u}{\partial y^2} + \frac{\partial^2 u}{\partial z^2} = -\frac{gS}{\nu + \nu_t} = \text{const} \quad (23)$$

in which  $\tau_{yx} = \rho(\nu + \nu_t)\partial u / \partial y$ ;  $\tau_{zx} = \rho(\nu + \nu_t)\partial u / \partial z$ ; and  $\nu$  = water kinematic viscosity. The above equation is the Poisson equation and can be solved by a conformal mapping method (White 1991, p. 115). That is, the orthogonals of the velocity contours can be used to delineate  $BG$  and  $CH$  in Fig. 1. Although the solution of Eq. (23) gives a laminar velocity profile, the orthogonals provide a first approximation of the boundary shear stress. According to the Schwarz–Christoffel transformation (Spiegel 1993, p. 204), the delimitation  $CH$  is found as (Guo 1998; Guo and Julien 2002)

$$\sin \frac{\pi y}{b} \cosh \frac{\pi z}{b} = 1 \quad (24)$$

which is identical to

$$\tan \frac{\pi y}{2b} = \exp\left(-\frac{\pi z}{b}\right) \quad (25a)$$

or

$$\frac{\pi y}{2b} = \tan^{-1} \exp\left(-\frac{\pi z}{b}\right) \quad (25b)$$

which is shown in Fig. 1.

### Average Bed Shear Stress

With reference to Fig. 1, after considering symmetry with respect to the channel centerline, the area  $A_b$  can be estimated as follows:

$$A_b = 2 \int_0^h y dz = \frac{4b}{\pi} \int_0^h \tan^{-1} \exp\left(-\frac{\pi z}{b}\right) dz \quad (26)$$

Expanding the integrand of Eq. (26) in terms of  $\exp(-\pi z/b)$  and integrating it yields

$$\begin{aligned} A_b &= \frac{4b^2}{\pi^2} \left( -(t-1) + \frac{t^3-1}{3^2} - \frac{t^5-1}{5^2} + \frac{t^7-1}{7^2} - \dots \right) \\ &= \frac{4b^2}{\pi^2} \sum_{n=1}^{\infty} (-1)^n \frac{t^{2n-1}-1}{(2n-1)^2} \end{aligned} \quad (27)$$

in which  $t = \exp(-\pi h/b)$ . Substituting Eq. (27) into Eq. (21b) gives the average bed shear stress as

$$\frac{\bar{\tau}_b}{\rho g h S} = \frac{4}{\pi^2} \frac{b}{h} \sum_{n=1}^{\infty} (-1)^n \frac{t^{2n-1}-1}{(2n-1)^2} \quad (28)$$

which is the first approximation of the average bed shear stress.

### Average Side-Wall Shear Stress

The area  $A_w$  corresponding to the side walls can be found by

$$A_w = bh - A_b \quad (29)$$

Substituting Eq. (27) into the above gives that

$$A_w = bh \left[ 1 - \frac{4}{\pi^2} \frac{b}{h} \sum_{n=1}^{\infty} (-1)^n \frac{t^{2n-1}-1}{(2n-1)^2} \right] \quad (30)$$

Furthermore, the average side-wall shear stress  $\bar{\tau}_w$  from Eq. (22b) becomes

$$\frac{\bar{\tau}_w}{\rho g h S} = \frac{A_w}{2h^2} = \frac{b}{2h} \left[ 1 - \frac{4}{\pi^2} \frac{b}{h} \sum_{n=1}^{\infty} (-1)^n \frac{t^{2n-1}-1}{(2n-1)^2} \right] \quad (31a)$$

or

$$\frac{\bar{\tau}_w}{\rho g h S} = \frac{b}{2h} \left( 1 - \frac{\bar{\tau}_b}{\rho g h S} \right) \quad (31b)$$

in which  $\bar{\tau}_b/(\rho g h S)$  is estimated by Eq. (28).

### Second Approximation with Correction Factors

The first approximation also implies that the maximum velocity occurs at the water surface. However, experiments (Tracy 1965; Imamoto and Ishigaki 1988; Nezu and Nakagawa 1993, p. 98) and numerical simulations (Naot and Rodi 1982) showed that in narrow channels, the maximum velocity occurs below the water

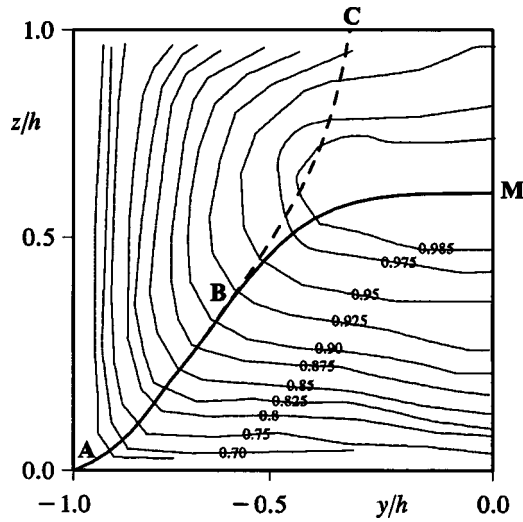


**Fig. 3.** Comparison of model delimitation with measured delimitation where  $b/h=2$  [line  $ABM$  is measured according to Nezu and Nakagawa (1993, p. 98), and dashed line  $ABC$  is first approximation]

surface, shown in Fig. 3. This is called the velocity dip phenomenon that is caused by secondary currents (Graf 1971, p. 107; Chiu and Chiou 1986). The second approximation aims at improving upon the first approximation by introducing two lumped empirical correction factors in the first approximation.

Substituting Eq. (26) into Eq. (21b) gives

$$\frac{\bar{\tau}_b}{\rho ghS} = \frac{4}{\pi} \frac{1}{h} \int_0^h \tan^{-1} \exp\left(-\frac{\pi z}{b}\right) dz \quad (32)$$

Applying the theorem of integration by parts to the above gives

$$\frac{\bar{\tau}_b}{\rho ghS} = \frac{4}{\pi} \tan^{-1} \exp\left(-\frac{\pi h}{b}\right) + \frac{4}{bh} \int_0^h \frac{z \exp(-\pi z/b)}{1 + \exp(-2\pi z/b)} dz \quad (33)$$

Considering that  $1 \leq 1 + \exp(-2\pi z/b) \leq 2$ , one may approximate the second term of Eq. (33) as

$$\begin{aligned} \int_0^h \frac{z \exp(-\pi z/b)}{1 + \exp(-2\pi z/b)} dz &\sim \int_0^h z \exp\left(-\frac{\pi z}{b}\right) dz \\ &\sim h \cdot (\lambda h) \exp\left(-\frac{\pi \lambda h}{b}\right) \end{aligned} \quad (34)$$

in which the mean value theorem for integrals has been applied and  $0 < \lambda < 1$ .

To include the effects of secondary currents, variable eddy viscosity and other possible effects, two lumped empirical correction factors  $\lambda_1$  and  $\lambda_2$  are introduced in Eq. (34). In other words, from Eqs. (33) and (34) one can assume

$$\frac{\bar{\tau}_b}{\rho ghS} = \frac{4}{\pi} \tan^{-1} \exp\left(-\frac{\pi h}{b}\right) + \frac{\lambda_1 h}{b} \exp\left(-\frac{\pi \lambda_2 h}{b}\right) \quad (35)$$

Substituting Eq. (35) into Eq. (31b) gives the second approximation for the average side-wall shear stress

$$\frac{\bar{\tau}_w}{\rho ghS} = \frac{b}{2h} \left[ 1 - \frac{4}{\pi} \tan^{-1} \exp\left(-\frac{\pi h}{b}\right) - \frac{\lambda_1 h}{b} \exp\left(-\frac{\pi \lambda_2 h}{b}\right) \right] \quad (36)$$

To ensure the validation of the above two equations in both narrow and wide channels, one can choose one condition from narrow channel and one-condition from wide channel to determine the values of  $\lambda_1$  and  $\lambda_2$ . According to Knight et al. (1984), for  $b/h=2$  (narrow channel), the experiments showed that the average bed shear stress  $\bar{\tau}_b$  is approximately equal to the average side-wall shear stress  $\bar{\tau}_w$ . Thus, one assumes

$$\bar{\tau}_b = \bar{\tau}_w \text{ at } b/h=2 \quad (37)$$

On the other hand, according to Knight et al. (1984), when  $b/h \rightarrow \infty$  (wide channel), one has

$$\frac{\bar{\tau}_w}{\rho ghS} = 0.61 \quad (38)$$

To incorporate the condition Eq. (38), one can consider Eq. (36) for the case  $b/h \rightarrow \infty$ . Since

$$\begin{aligned} \frac{4}{\pi} \tan^{-1} \exp\left(-\frac{\pi h}{b}\right) &\rightarrow \frac{4}{\pi} \tan^{-1} \left(1 - \frac{\pi h}{b}\right) \\ &\rightarrow \frac{4}{\pi} \left(\frac{\pi}{4} - \frac{\pi h}{2b}\right) = 1 - \frac{2h}{b} \end{aligned} \quad (39)$$

and

$$\frac{\lambda_1 h}{b} \exp\left(-\frac{\pi \lambda_2 h}{b}\right) \rightarrow \frac{\lambda_1 h}{b} \quad (40)$$

substituting the above two relations into Eq. (36) gives

$$\frac{\bar{\tau}_w}{\rho ghS} \rightarrow \frac{b}{2h} \left[ 1 - \left(1 - \frac{2h}{b}\right) - \frac{\lambda_1 h}{b} \right] = 1 - \frac{1}{2} \lambda_1 \quad (41)$$

Combining Eq. (38) and Eq. (41) yields

$$\lambda_1 = 0.78 \approx \frac{\pi}{4} \quad (42)$$

Applying the condition Eq. (37) in Eqs. (35) and (36) at  $b/h=2$ , one has

$$\frac{4}{\pi} \tan^{-1} \exp\left(-\frac{\pi}{2}\right) + \frac{\pi}{8} \exp\left(-\frac{\pi \lambda_2}{2}\right) = \frac{1}{2} \quad (43)$$

in which Eq. (42) has been applied. Solving the above equation gives

$$\lambda_2 = 0.316 \approx \frac{1}{\pi} \quad (44)$$

Finally, with Eqs. (42) and (44), the second approximation of the average bed shear stress Eq. (35) reduces to

$$\frac{\bar{\tau}_b}{\rho ghS} = \frac{4}{\pi} \tan^{-1} \exp\left(-\frac{\pi h}{b}\right) + \frac{\pi h}{4b} \exp\left(-\frac{h}{b}\right) \quad (45)$$

and the side-wall shear stress Eq. (36) reduces to

$$\frac{\bar{\tau}_w}{\rho ghS} = \frac{b}{2h} \left[ 1 - \frac{4}{\pi} \tan^{-1} \exp\left(-\frac{\pi h}{b}\right) - \frac{\pi h}{4b} \exp\left(-\frac{h}{b}\right) \right] \quad (46)$$

One can demonstrate that for a very wide channel where  $b/h \rightarrow \infty$ , the second term of Eq. (45) vanishes and  $\tan^{-1} 1 = \pi/4$ , which reduces Eq. (45) to  $\bar{\tau}_b \rightarrow \rho ghS$ . This coincides with the result in a two-dimensional flow. However, the average side-wall shear stress Eq. (46) for large width-depth ratios is not zero, which can be clearly seen from Eq. (41).



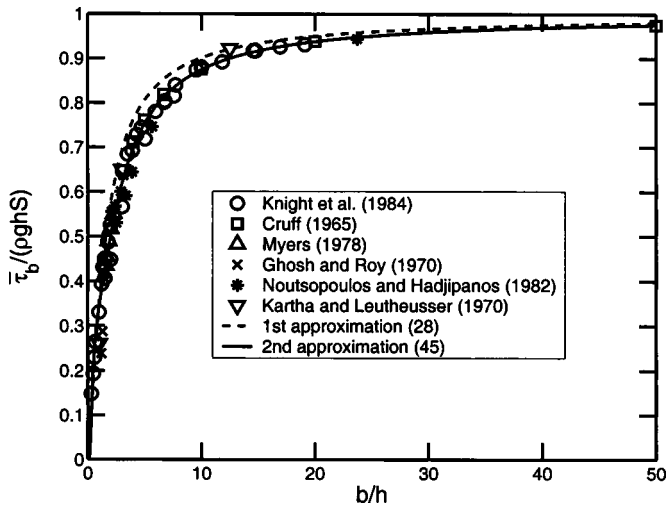


Fig. 4. Comparison of first approximation and second approximation for average bed shear stress with experimental data

### Comparison with Experimental Data

The existing experimental data in smooth open channels have been well documented by Knight et al. (1984). This data set includes those of Cruff (1965), Ghosh and Roy (1970), Kartha and Leutheusser (1970), Myers (1978), Knight and Macdonald (1979), and Noutsopoulos and Hadjipanos (1982). In terms of the average bed shear stress, comparison between Eq. (28) and the experimental measurements is shown in Fig. 4 with the dashed line. One can see that the first approximation Eq. (28) slightly overestimates the average bed shear stress. This demonstrates that except for gravity, the effects of secondary currents and interface shear stress should be considered at least empirically. The second approximation Eq. (45), denoted with the solid line, agrees very well with the experimental data. The correlation coefficient between Eq. (45) and the data is about 0.994. If one defines the relative error as

$$\text{err} = \left| \frac{\text{calculated} - \text{measured}}{\text{measured}} \right| \quad (47)$$

then the average relative error is about 5.6%. If the three largest relative errors are excluded, then the average relative error reduces to 3.1%.

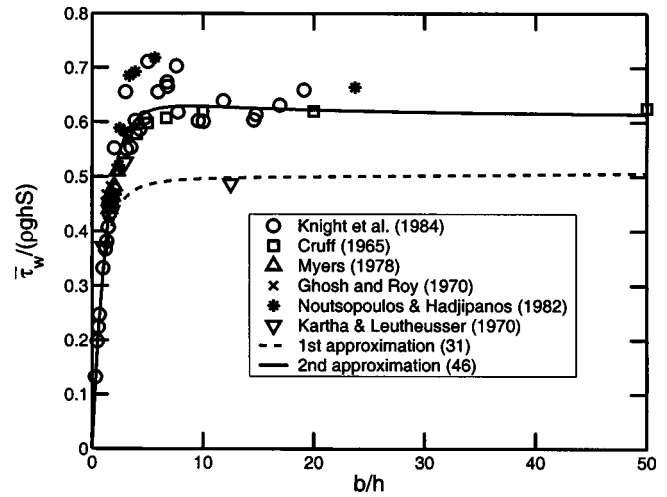


Fig. 5. Comparison of first approximation and second approximation for average side-wall shear stress with experimental data

In terms of the side-wall shear stress, comparison between the first approximation Eq. (31a) and the measurements of Knight et al. (1984) is shown in Fig. 5. Unlike those of the average bed shear stress, the first approximation, denoted with the dashed line, is 17% less than the experimental data when the width–depth ratio becomes large. This shows that the first approximation is not good for the average side-wall shear stress. However, the second approximation Eq. (46) improves the first approximation greatly, as denoted with the solid line in Fig. 5.

### Implication to Flume Velocity Profile Study

Traditionally the bed shear velocity is determined by fitting the near bed velocity profile to the logarithmic law when studying turbulent velocity profiles in flume experiments (Nezu and Nakagawa 1993). Eq. (45), which is independent of velocity profiles, can simplify this process in smooth rectangular flumes. Table 1 examines this application where the measured values were reported in literature (Coleman 1986; Lyn 1986, 2000; Muste and Patel 1997), and the calculated values are from Eq. (45) according to  $u_{*b} = \sqrt{\bar{\tau}_b / \rho}$ . Note that the three data sources are independent of those in Fig. 4. One can see that the measured shear velocities are slightly larger than those from Eq. (45). This is because the mea-

Table 1. Comparison of Calculated Bed Shear Velocities with Measurements in Smooth Flumes

Parameter	Coleman's (1986)	Lyn's (1986, 2000)				Muste and Patel's (1997)		
	Run 1	C1	C2	C3	C4	CW01	CW02	CW03
Slope $S$ ( $\times 10^{-3}$ )	2.00	2.06	2.70	2.96	4.01	0.739	0.768	8.13
Temperature $T$ ( $^{\circ}\text{C}$ )	21.1	18.7	21.3	21.0	21.3	18.4	17.2	17.4
Depth $h$ (cm)	17.2	6.54	6.53	5.75	5.69	13.00	12.8	12.70
Average velocity $V$ (m/s)	1.050	0.658	0.772	0.734	0.868	0.624	0.628	0.634
Hydraulic radius $R$ (cm)	8.75	4.39	4.38	4.02	3.99	10.10	10.00	9.90
Reynolds number $R = VR/\nu$ ( $\times 10^4$ )	9.17	2.73	3.41	2.96	3.50	6.00	5.80	5.80
Froude number $F = V/\sqrt{gh}$	0.80	0.82	0.97	0.97	1.16	0.55	0.56	0.57
Width–depth ratio $b/h$	2.00	4.08	4.09	4.64	4.69	7.00	7.10	7.16
Bed shear velocity $u_{*b}$ (cm/s), from Eq. (45)	4.14	3.05	3.49	3.50	4.06	2.78	2.82	2.89
Measured shear velocity $u_{*b}$ (cm/s)	4.10	3.10	3.70	3.60	4.30	2.92	2.92	2.98

sured values are local shear velocities while the calculated are the average bed shear velocities. In general, the calculated values are considered comparable with those reported in the literature.

## Summary and Conclusions

This analysis defines the average bed and sidewall shear stresses for steady uniform flow in smooth rectangular channels. An analysis of the continuity and momentum equations yields a formulation for average bed shear stress in Eq. (18) and average sidewall shear stress in Eq. (20). Both formulations show the importance of three main terms in the shear stress analysis: (1) a gravitational term; (2) a secondary flow term; and (3) a shear stress term at the interface. An analytical solution is possible for the case where the eddy viscosity is constant and secondary flows are negligible. This analytical solution is obtained after considering the Schwarz–Christoffel transformation. This leads to the first approximation in terms of series expansion for the bed shear stress in Eq. (28) and sidewall shear stress in Eq. (31).

When comparing with experimental measurements in Fig. 4, this first approximation slightly overestimates the measured average bed shear stresses. Most important is that in Fig. 5, the first approximation underestimates the side-wall shear stress measurements by about 17% when the channel width–depth ratio is large. A second approximation is then proposed after introducing two empirical coefficients. The second approximation [Eqs. (45) and (46)] yields a better agreement with the experimental measurements with  $R^2 > 0.99$  and an average relative error less than 6% for the average bed shear stress. This second approximation is therefore recommended in practice.

## Acknowledgments

The writers thank the two anonymous reviewers and Associate Editor Professor D. A. Lyn for their critical and constructive comments.

## Notation

The following symbols are used in this paper:

- $A$  = area of control volume surface;
- $A_b, A_w$  = areas corresponding to bed shear stress and side-wall shear stress, respectively;
- $b$  = width of channel;
- $F$  = Froude number;
- $g$  = gravitational acceleration;
- $h$  = flow depth;
- $l$  = integration length;
- $\mathbf{n}$  = normal vector pointing outside of control volume;
- $R$  = global Reynolds number;
- $R$  = hydraulic radius or correlation coefficient;
- $S$  = channel slope;
- $T$  = temperature ( $^{\circ}\text{C}$ );
- $t$  = interim variable  $t = \exp(-\pi h/b)$ ;
- $u$  = downstream flow velocity in  $x$  direction;
- $u_{*b}$  = average bed shear velocity;
- $\mathcal{V}$  = average velocity of cross section;
- $V$  = volume of control volume;
- $v$  = velocity in lateral direction  $y$ ;
- $w$  = velocity in  $z$  direction;

- $x$  = coordinate of downstream flow direction;
- $y$  = coordinate of lateral direction;
- $z$  = coordinate that is perpendicular to flow direction  $x$  and lateral direction  $y$ ;
- $\beta$  = angle between coordinate  $z$  and normal vector  $\mathbf{n}$  pointing outside of control volume;
- $\theta$  = angle of channel slope  $S = \sin \theta$ ;
- $\lambda, \lambda_1, \lambda_2$  = correction factors;
- $\nu, \nu_t$  = kinematic viscosity of water and eddy viscosity, respectively;
- $\rho$  = mass density of water;
- $\bar{\tau}_b, \bar{\tau}_w$  = average bed shear stress and side-wall shear stress, respectively; and
- $\tau_{yx}, \tau_{zx}$  = shear stresses in flow direction  $x$  applied on  $z-x$  plane and  $y-x$  plane, respectively.

## References

- Babaeyan-Koopaei, K., Ervine, D. A., Carling, P. A., and Cao, Z. (2002). "Velocity and turbulence measurements for two overbank flow events in River Severn." *J. Hydraul. Eng.*, 128(10), 891–900.
- Berlamont, J. E., Trouw, K., and Luyckx, G. (2003). "Shear stress distribution in partially filled pipes." *J. Hydraul. Eng.*, 129(9), 697–705.
- Bocchiola, D., Menduni, G., and Ward, D. (2003). "Testing block probes for wall shear stress measurement in water flows." *J. Hydraul. Eng.*, 129(1), 102–109.
- Cheng, N. S. (2002). "Exponential formula for bedload transport." *J. Hydraul. Eng.*, 128(10), 942–946.
- Chien, N., and Wan, Z. H. (1999). *Mechanics of sediment transport*, ASCE, New York.
- Chiu, C. L., and Chiou, J. D. (1986). "Structure of 3-D flow in rectangular open-channels." *J. Hydraul. Eng.*, 112(11), 1050–1068.
- Chiu, C. L., and Lin, G. F. (1983). "Computation of 3-D flow and shear in open channels." *J. Hydraul. Eng.*, 109(11), 1424–1440.
- Coleman, N. L. (1986). "Effects of suspended sediment on the open-channel velocity distribution." *Water Resour. Res.*, 22(10), 1377–1384.
- Cruff, R. W. (1965). "Cross-channel transfer of linear momentum in smooth rectangular channels." *Water-Supply Paper, 1592-B*, U.S. Geological Survey, Center, Miss., B1–B26.
- Einstein, H. A. (1942). "Formulas for the transportation of bed-load." *Trans. Am. Soc. Civ. Eng.*, 107, 561–597.
- Ghosh, S. N., and Roy, N. (1970). "Boundary shear distribution in open-channel flow." *J. Hydraul. Div., Am. Soc. Civ. Eng.*, 96(4), 967–994.
- Graf, W. (1971). *Hydraulics of sediment transport*, McGraw-Hill, New York.
- Guo, J. (1998). "Turbulent velocity profiles in clear water and sediment-laden flows." PhD dissertation, Colorado State Univ., Fort Collins, Colo.
- Guo, J. (1999). "Discussion of Mechanism of energy transportation and turbulent flow in a 3D channel by S. Q. Yang and S. Y. Lim." *J. Hydraul. Eng.*, 125(3), 319–320.
- Guo, J., and Julien, P. Y. (2001). "Turbulent velocity profiles in sediment-laden flows." *J. Hydraul. Res.*, 39(1), 11–23.
- Guo, J., and Julien, P. Y. (2002). "Boundary shear stress in smooth rectangular open-channels." *Advances in Hydraulics and Water Engineering, Proc. 13th IAHR-APD Congress*, Vol. 1, Singapore, 76–86.
- Hu, C. H. (1985). The effect of the width/depth ratio and side-wall roughness on velocity profile and resistance in rectangular open-channels. MS thesis, Tsinghua Univ., Beijing.
- Imamoto, H., and Ishigaki, T. (1988). "Measurements of secondary flow in an open channel." *Proc., 6th IAHR-APD Congress*, Kyoto, Japan, 513–520.
- Johnson, W. (1942). "The importance of side-wall friction in bed-load investigation." *Civ. Eng. (N.Y.)*, 12, 329–331.



- Julien, P. Y. (1995). *Erosion and sedimentation*, Cambridge University Press, Cambridge, U.K.
- Kartha, V. C., and Leutheusser, H. J. (1970). "Distribution of tractive force in open-channels." *J. Hydraul. Div., Am. Soc. Civ. Eng.*, 96(7), 1469–1483.
- Keulegan, G. H. (1938). "Laws of turbulent flow in open-channels." *Natl. Bur. Stand. Circ. (U. S.)*, 21, 709–741.
- Knight, D. W. (1981). "Boundary shear in smooth and rough channels." *J. Hydraul. Div., Am. Soc. Civ. Eng.*, 107(7), 839–851.
- Knight, D. W., Demetriou, J. D., and Homed, M.E. (1984). "Boundary shear in smooth rectangular channels." *Agric. Water Manage.*, 110(4), 405–422.
- Knight, D. W., and MacDonald, J. A. (1979). "Open-channel flow with varying bed roughness." *J. Hydraul. Div., Am. Soc. Civ. Eng.*, 105(9), 1167–1183.
- Leighly, J. B. (1932). "Toward a theory of the morphologic significance of turbulence in the flow of water in streams." *Univ. of Calif. Publ. Geography*, 6(1), 1–22.
- Lundgren, H., and Jonsson, I. G. (1964). "Shear and velocity distribution in shallow channels." *J. Hydraul. Div., Am. Soc. Civ. Eng.*, 90(1), 1–21.
- Lyn, D. A. (1986). "Turbulence and turbulent transport in sediment-laden open-channel flows." *Rep.*, W. M. Keck Laboratory of Hydraulics and Water Resources, California Institute of Technology, Pasadena, Calif.
- Lyn, D. A. (2000). "Regression residuals and mean profiles in uniform open-channel flows." *J. Hydraul. Eng.*, 126(1), 24–32.
- Muste, M., and Patel, V. C. (1997). "Velocity profiles for particles and liquid in open-channel flow with suspended sediment." *J. Hydraul. Eng.*, 123(9), 742–751.
- Myers, W. R. C. (1978). "Momentum transfer in a compound channel." *J. Hydraul. Res.*, 16(2), 139–150.
- Naot, D., and Rodi, W. (1982). "Calculation of secondary currents in channel flow." *J. Hydraul. Div., Am. Soc. Civ. Eng.*, 108(8), 948–968.
- Nezu, I., and Nakagawa, H. (1993). "Turbulence in open-channel flows." *IAHR Monograph Series*, A. A. Balkema, Rotterdam, The Netherlands.
- Noutsopoulos, G. C., and Hadjipanos, P. A. (1982). "Discussion of Boundary shear in smooth and rough channels by D. W. Knight." *J. Hydraul. Div., Am. Soc. Civ. Eng.*, 108(6), 809–812.
- Spiegel, M. R. (1993). *Complex variables*, McGraw-Hill, New York.
- Tracy, H. J. (1965). "Turbulent flow in a three-dimensional channel." *J. Hydraul. Div., Am. Soc. Civ. Eng.*, 91(6), 9–35.
- White, F. M. (1991). *Viscous fluid flow*, McGraw-Hill, New York.
- Yang, S. Q., and Lim, S. Y. (1997). "Mechanism of energy transportation and turbulent flow in a 3D channel." *J. Hydraul. Eng.*, 123(8), 684–692.
- Yang, S. Q., and Lim, S. Y. (1998). "Boundary shear stress distributions in smooth rectangular open channel flows." *Proc. Inst. Civ. Eng., Waters. Maritime Energ.*, 130(3), 163–173.